(Preprint) AAS 18-416

PRELIMINARY INTERPLANETARY MISSION DESIGN AND NAVIGATION FOR THE DRAGONFLY NEW FRONTIERS MISSION CONCEPT

Christopher J. Scott[*], Martin T. Ozimek[*], Douglas S. Adams[†], Ralph D. Lorenz[‡], Shyam Bhaskaran[§], Rodica Ionasescu[¶], Mark Jesick[¶], and Frank E. Laipert[¶]

Dragonfly is one of two mission concepts selected in December 2017 to advance into Phase A of NASA's New Frontiers competition. Dragonfly would address the Ocean Worlds mission theme by investigating Titan's habitability and prebiotic chemistry and searching for evidence of chemical biosignatures of past (or extant) life. A rotorcraft lander, Dragonfly would capitalize on Titan's dense atmosphere to enable mobility and sample materials from a variety of geologic settings. This paper describes Dragonfly's baseline mission design giving a complete picture of the inherent tradespace and outlines the design process from launch to atmospheric entry.

INTRODUCTION

Hosting the moons Titan and Enceladus, the Saturnian system contains at least two unique destinations that have been classified as ocean worlds. Titan, the second largest moon in the solar system behind Ganymede and the only planetary satellite with a significant atmosphere, is larger than the planet Mercury at 5,150 km (3,200 miles) in diameter. Its atmosphere, approximately 10 times the column mass of Earth's, is composed of 95% nitrogen, 5% methane, 0.1% hydrogen along with trace amounts of organics.[1] Titan's atmosphere may resemble that of the Earth before biological processes began modifying its composition. Similar to the hydrological cycle on Earth, Titan's methane evaporates into clouds, rains, and flows over the surface to fill lakes and seas, and subsequently evaporates back into the atmosphere. Beneath its surface, Titan likely contains a briney, global ocean under a layer of ice.[2] Interestingly, on Titan, water plays the role of magma on Earth and methane plays the role of water. Because of its similarities with an early Earth, complex and active organic chemistry, internal water ocean as well as liquid water on the surface in the past, and a possible model for a future Earth, Titan is a compelling destination of high astrobiological value.[3]

Titan has been considered many times in the past as a potential destination for robotic exploration. As technology and our knowledge of Titan has advanced over the last few decades a plethora of mission concepts have been explored including entry probes, penetrators, sounding rockets, balloons, dirigibles, landers, and even submarines.[4] More recently, the Johns Hopkins Applied Physics Laboratory (APL) was a central partner in the team that developed the Titan Mare Explorer (TiME) concept (a floating, lake lander),[5] led a 2007 NASA Titan Flagship Mission Study[6] and was a contributing institution for the Planetary Decadal Survey Titan Saturn System Mission Concept Study.[7] Although rotorcraft have previously been identified as an enabler on Titan,[4] advances in multi-rotor drones have led to simpler mechanical implementations, compact sensors, and reliable autonomy that can be applied to drone-like, planetary landers. The 2007 flagship study called for a multi-vehicle solution which included an orbiter, a hot-air balloon, and a lander. Dragonfly would

[*]Mission Design Engineer, Space Exploration Sector, Johns Hopkins University, 11101 Johns Hopkins Road, Laurel, Maryland 20723.
[†]System Engineer, Space Exploration Sector, Johns Hopkins University, 11100 Johns Hopkins Road, Laurel, Maryland 20723.
[‡]Project Scientist, Space Exploration Sector, Johns Hopkins University, 11100 Johns Hopkins Road, Laurel, Maryland 20723.
[§]Supervisor, Outer Planets Navigation Group, California Institute of Technology, 4800 Oak Grove Drive, Pasadena CA, 91109.
[¶]Navigation Engineer, Jet Propulsion Laboratory, California Institute of Technology, 4800 Oak Grove Drive, Pasadena CA, 91109.

achieve most of the science objectives of at least two of the three principle elements (lander and hot-air balloon) on a New Frontiers budget by the paradigm-shifting utilization of modern rotocraft technology.

The goal of the Dragonfly interplanetary mission design and navigation is to deliver the entry vehicle to the Titan atmospheric interface condition. This condition must target the selected landing site while judiciously balancing the use of system resources and risk. Due to the low gravity, the density of Titan's atmosphere decreases slowly with altitude compared to those of Venus, Earth, or Mars. This characteristic stretches the typical time and distance scales associated with atmospheric entry and eliminates the need for a shallow approach into the atmosphere. Dragonfly enters Titan's atmosphere directly from interplanetary space before landing. Eliminating the need for large maneuvers, flybys of Titan, or aerocapture, direct entry dramatically simplifies the mission design and operations prior to landing.

An overarching theme of the trajectory design is simplicity in terms of both the trajectory and operations. As described in the following sections, the low deterministic post-launch Δv interplanetary trajectory possesses nearly constant arrival conditions throughout both the primary and backup launch periods. For a given arrival asymptote with respect to Saturn, the locus of all possible Titan entry conditions is determined semi-analytically which ultimately bounds accessible areas on the surface. Acceptable designs must reach the target landing site and allow sufficient time between landing and Earthset (for communication) while satisfying the aerothermal heating, and acceleration requirements of the entry system.

This paper outlines the major mission design trades and relevant theory from launch to atmospheric entry. First, the interplanetary trade space is introduced in the context of the design parameters which constrain the space of all feasible designs. The performance of a variety of launch vehicles is tabulated including launch capability and delivered mass into the Saturnian system. Arrival conditions upon entry into the Saturnian system and thus Titan entry conditions are coupled to the interplanetary trajectory type, time-of-flight, and launch energy. The next section mathematically describes the relationships between the Saturnian system entry condition and the space of all Titan arrival conditions including entry speed, entry flight-path-angle (EFPA), target latitude and longitude, arrival time, and time to Earthset. These conditions are mapped to parameters which directly influence the Thermal Protection System (TPS) design such as heat flux, heat load, and stagnation pressure, in addition to the peak acceleration experienced by the entry system. Lastly, a description of the navigation strategy is introduced with a high-level introduction of the pragmatic design flow among mission design, navigation, and atmospheric descent modeling. A detailed analysis of the entry and descent strategy and modeling will be provided in a future publication.

The full end-to-end baseline trajectory is developed by a multi-institutional mission design and navigation team. (See Figure 1.) A team at APL derives an optimized high-fidelity interplanetary trajectory to the Saturn-Titan system based on a set of mission constraints. The Saturn incoming hyperbolic excess velocity (v_∞) analytically maps to site selection accessibility. A navigation team at the Jet Propulsion Laboratory (JPL) analyzes the orbit determination uncertainties of the selected trajectory subject to a ground-based radiometric observation campaign and associated spacecraft hardware uncertainties such as maneuver execution errors. This analysis influences a set of atmospheric entry simulations led by a team at NASA's Langley Research Center (LaRC) using the Program to Optimize Simulated Trajectories (POST-II) software, creating a landing ellipse on the surface. This analysis can inform entry vehicle hardware adjustments by NASA Ames and LaRC. The entire process iterates until a nominal interplanetary trajectory is selected that guides the Dragonfly entry vehicle to a feasible landing footprint across an entire launch period.

INTERPLANETARY TRANSFER

Broad Search for Enabling Interplanetary Trajectories

The interplanetary trajectory is subject to the constraints listed in Table 1. The launch, cruise, and gravity assist constraints drive the interplanetary search space independent of Titan entry, while the subsequent entry constraints functionally depend on the arrival $\mathbf{v}_\infty$ into the Saturnian system. This section covers the first three blocks in Figure 1. A patched conics broad search was performed over the entire baseline launch period over the 2025 calendar year in addition to the backup 2026 calendar year. The goal of the broad search was to obtain a mass-optimal baseline and backup pair such that the worst-case mass of the pair is highest

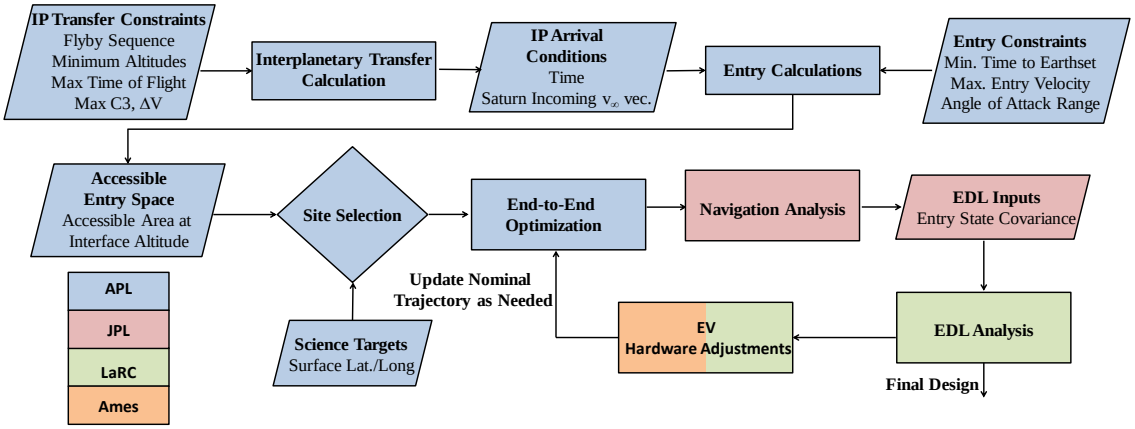

Figure 1. Trajectory design process.

Table 1. Dragonfly trajectory constraint drivers.

Affected Phase	Reason for Constraint	Constraint Name	Condition	Converged Value*
Launch	Schedule/AO Requirement	Baseline Departure date	$1/1/2025 - 12/31/2025$	$4/12/2025 - 5/2/2025$
Launch * Schedule	Backup launch date	6-18 months after baseline date		
Launch	Launch vehicle provider	Launch declination (DLA)	$-28.5° \leq$ DLA $\leq 28.5°$	$21.8°$
Launch	Cost	Launch vehicle	Atlas V-411 or equivalent	
Cruise	Cost	Time-of-Flight	≤ 11 years	9.7 years
Gravity Assists	Thermal	Venus Closest Approach Altitude	≥ 300 km	4000 km
Gravity Assists	Probability of Impact	Earth Closest Approach Altitude	≥ 1000 km	$\{1134, 1409, 1002\}$ km
Entry	TPS Design	Deceleration	< 12 Earth g's^2	11.9 Earth g's
Entry	TPS Design	Nominal Heat Flux	< 300 W/cm^2(goal)	146 W/cm^2
Entry	TPS Design	Nominal Heat Load	$< 10,000$ J/cm^2	$9,460$ J/cm^2
Entry	Communications	Time to First Earth-Set	> 61 hours	Satisfied

* Driving parameters across 20-day launch period and entry dispersions.

with respect to all alternative solution pairs. Gravity assists of Earth, Venus, and Mars were included with a patched conics assumption. Jupiter was immediately discarded as it is out of phase during the desired time period. Possible trajectory arcs between gravity assist bodies included non-resonant ballistic transfers, v_∞-leveraging arcs,[8] and even-π resonant returns.[9]

The results of the interplanetary trajectory broad search appear in Figure 2, assuming a monopropellant main engine specific impulse of 230 seconds, and launch performance consistent with the NASA NLS-II launch vehicle contract. The Atlas V-411 was selected as a representative launch vehicle as it lies within the medium performance launch vehicle class as specified in the AO. On the basis of selecting an optimal pair of primary and backup trajectories that satisfies all mission constraints, a 2025 EVEE is paired with a 2026 VEE. The 2025 EVEE is equivalent to the 2026 VEE with a prepended 1:1 Earth resonance. Since both trajectories are geometrically equivalent from the 2026 Earth encounter or launch for the baseline and backup respectively, it is possible to maintain the exact same terminal phases for Titan encounter, vastly simplifying navigational and operational planning. Adding the option for the equivalent mission a year later provides significant advantages including schedule flexibility, a shorter time-of-flight, and less multi-mission radioisotope thermolelectric generator (MMRTG) degradation after launch. In fact, this pairing of trajectories repeats again in 2027 and 2028 with qualitatively similar arrival conditions at Titan, launch costs, and Δv requirements. For the EVEE sequence, the acronyms EGA0, EGA1, and EGA2 are used to denote the first, second, and third Earth gravity assists respectively, and VGA1 denotes the Venus gravity assist. This naming convention remains the same for the 2026 VEE trajectory with the exception of EGA0 which is eliminated from the sequence, instead becoming equivalent to the Earth launch.

With the 2025 EVEE and 2026 VEE pair selected as the optimal configuration, the total time-of-flight is

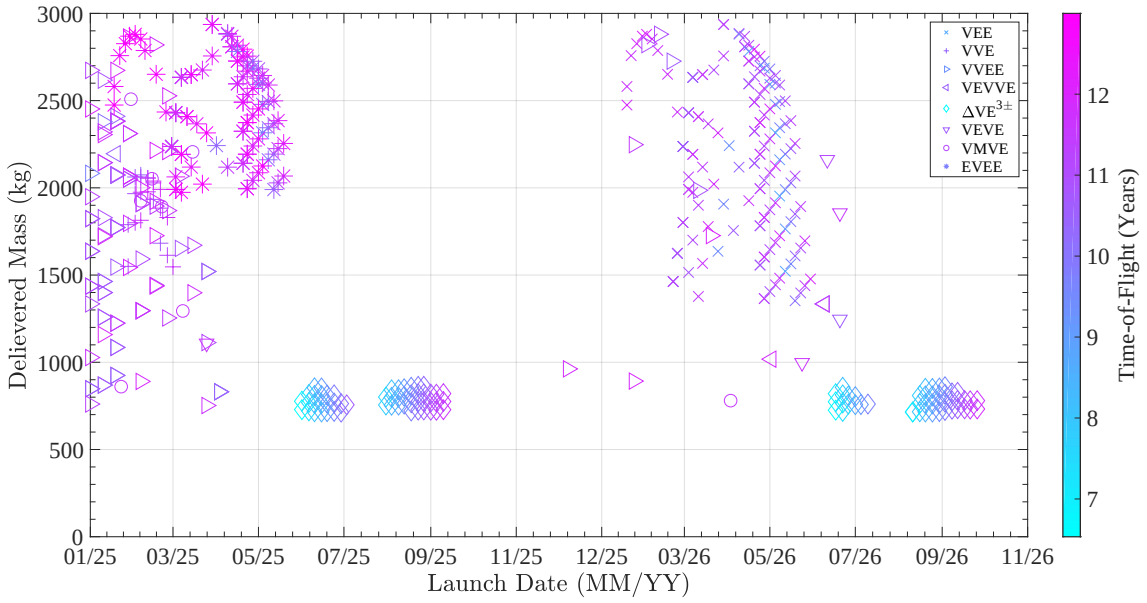

Figure 2. Broad search delivered mass capability on an Atlas V-411 launch vehicle. Solutions with time-of-flight $\leq$ 12 years are displayed.

minimized given the mission constraints. The most effective portion of the trajectory to minimize time-of-flight is on the transfer leg from the final Earth gravity assist (EGA2) to arrival in the Saturn-Titan system. This time reduction equates to piercing the Saturn-Titan system at lower heliocentric true anomalies, and therefore at higher arrival v_∞ to minimize the arrival date. Assuming that the entry vehicle can compensate for the increased v_∞, then the arrival date is fundamentally limited by the constraint on minimum Earth gravity assist altitude (Table 1), as shown in Figure 3.

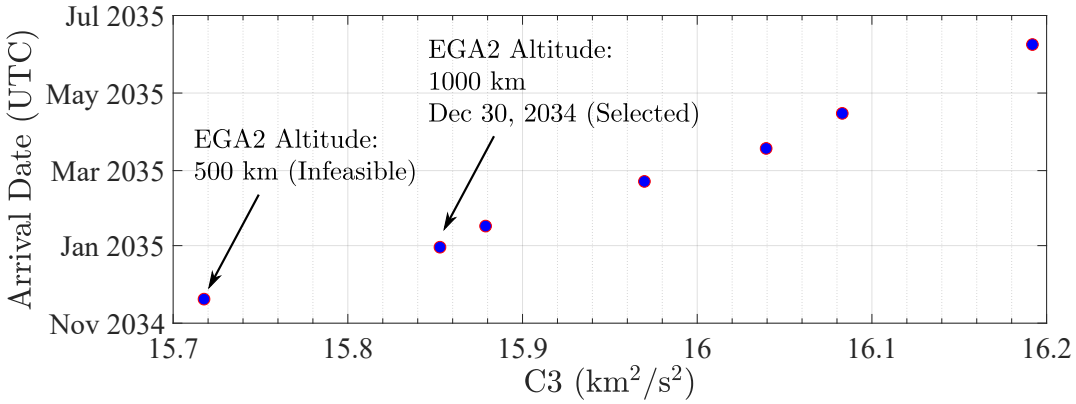

Figure 3. Arrival date versus C3 for the EVEE baseline interplanetary transfer.

Optimized High-Fidelity Solutions and Launch Period

Within the "End-to-End Optimization" block of Figure 1, all baseline and backup trajectories are converted from patched conics into a high-fidelity, numerically integrated force model in accordance with the specifications in Table 2. The entire trajectory is converged as part of one multiple shooting direct Δv

Table 2. High-fidelity force modeling settings for Dragonfly.

Phase	Central Body	Forces
Launch and Earth Gravity Assists	Earth	21x21 Earth Gravity Model (WGS84_EGM96) Point-Mass Perturbations: Sun, Moon
Venus Gravity Assist	Venus	21x21 Venus Gravity Model (MGNP180U) Point-Mass Perturbations: Sun,Earth-Moon System, Mercury
Interplanetary	Sun	Solar Point-Mass Gravity Point-Mass Perturbations: Mercury, Venus, Earth-Moon System, Mars, Jupiter System, Saturn System, Uranus System
Titan Arrival	Saturn	4x0 Titan Gravity Model (Zonals - J4) Point-Mass Perturbations: Sun, Jupiter System, Saturn

minimization problem solved with nonlinear programming (NLP). The optimization problem is established under the well-known formulation paradigm of control points at ephemeris bodies (e.g. launch, flyby, arrival) and breakpoints satisfying state continuity in heliocentric space.[10, 11, 12] The breakpoints exist between neighboring control points in time and are evaluated by forwards and backwards propagation emanating from the control points. The selected times for the breakpoints are fixed epochs that are approximately at the midpoint in time between neighboring control points. Additional control points also exist as heliocentric states on the EGA2 to Saturn-Titan system transfer to minimize sensitivity. Fully assembled, the trajectory optimization problem contains seven legs consisting of eight control points, two maneuvers to be optimized (launch injection and Titan targeting), and seven breakpoint constraints. Using this framework, the entire trajectory has been converged from a patched conics initial guess in Analytical Graphics' Systems Tool Kit® Astrogator module and in JPL's Monte toolset using the Computer Optimization System for Multiple Independent Courses (COSMIC) application. The preceding process is repeated at daily fixed launch epochs correspond-

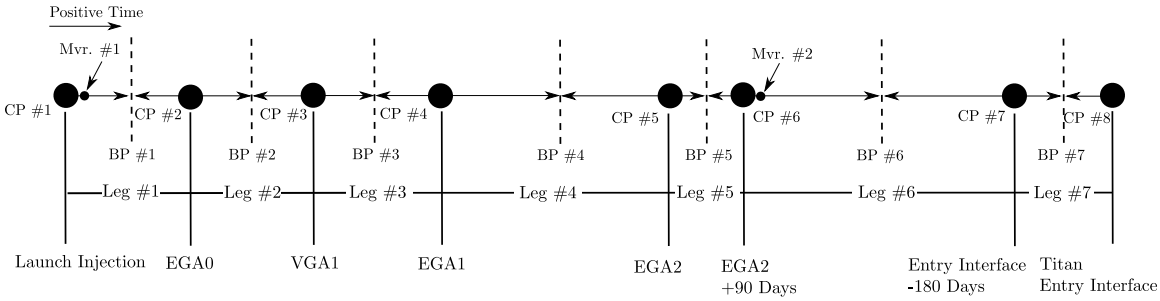

Figure 4. High-fidelity control point (CP), breakpoint (BP), and maneuver (Mvr.) transcription.

ing to daily launch opportunities. The arrival state at Titan entry interface is held inertially fixed and locked in time. Near the beginning of the launch period, the Titan targeting maneuver (i.e. Mvr. 2 in Figure 4) optimally reduces to zero through EGA2. However, on later days of the launch period, the effectiveness of the Earth gravity assist saturates due to the minimum altitude constraints being reached, and the Titan targeting reaches nonzero values to preserve the fixed entry interface state (see Figure 5).

SYSTEM ENTRY

Covering the "Entry Calculations", "Entry Constraints", and "Accessible Entry Space" blocks in Figure 1, this section describes the theory used to map the trade space of atmospheric entry conditions. The process used for landing site selection is beyond the scope of this paper. The analysis begins with an approach similar to that used to calculate dual satellite-aided capture solutions in the Jovian system.[13] Each interplanetary trajectory maps to a Saturn arrival time, t_o, and an incoming v_∞ vector. These in turn, map to a space of atmospheric entry conditions upon arrival to Titan.

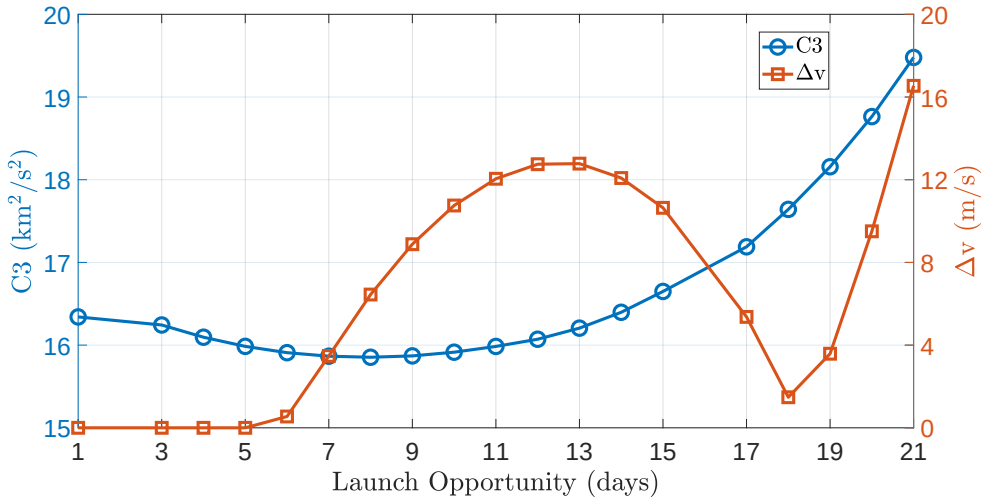

Figure 5. Dragonfly launch period performance over launch day. Due to the 1:1 Earth resonance, The baseline and backup launch periods have near-identical performance, varying only in declination of launch asymptote (DLA).

Table 3. Dragonfly trajectory constraint drivers.

Parameter	Baseline	Backup
Max. DLA (°)	21.8	6.8
Max. C3 (km^2/s^2)	19.9	19.9
Max. Post-Launch Δv (m/s)*	20.7	20.7
EGA0 Min. Flyby Alt. (km)	1134	N/A
VGA1 Min. Flyby Alt. (km)	4000	4000
EGA1 Min. Flyby Alt. (km)	1409	1409
EGA2 Min. Flyby Alt. (km)	1002	1002

* Deterministic value only considers Titan targeting and excludes Earth bias maneuvers that are the subject of future work.

Saturnian System Entry

Defining a reference frame where the x-y plane lies in the orbital plane of Titan, the incoming v_∞ vector with respect to Saturn can be expressed as

$$\mathbf{v}_\infty = v_\infty \begin{bmatrix} \cos\alpha\cos\delta & \sin\alpha\cos\delta & \sin\delta \end{bmatrix}^T \tag{1}$$

where α and δ are the right ascension and declination. The range of possible inclinations of the incoming hyperbola with respect to this plane is constrained to $\delta \leq i \leq \pi - \delta$. To encounter Titan, the incoming hyperbola must have a node crossing radius equal to the orbital radius of Titan at the time of entry. Using this constraint, the orbital elements of the incoming hyperbola can be calculated analytically for Titan entry before and after periapse, and for prograde and retrograde approach geometries with respect to Saturn. Also, the existence of Saturn-centered ascending and/or descending node encounter geometries can be calculated, see Appendix. Using the orbital elements, the velocity of the spacecraft with respect to Saturn at the node crossing, $\mathbf{v}_N$, can be calculated analytically. If at the instant of the node crossing Titan's velocity with respect to Saturn is $\mathbf{v}_T$, the v_∞ vector with respect to Titan is expressed as

$$\mathbf{v}_{T\infty} = \mathbf{v}_N - \mathbf{v}_T \tag{2}$$

To this point, the analysis has omitted phasing. Mathematically a position in Titan's orbit must be mapped to a time and to a set of spacecraft orbital elements. To first order we assume that the Titan arrival time, t_e

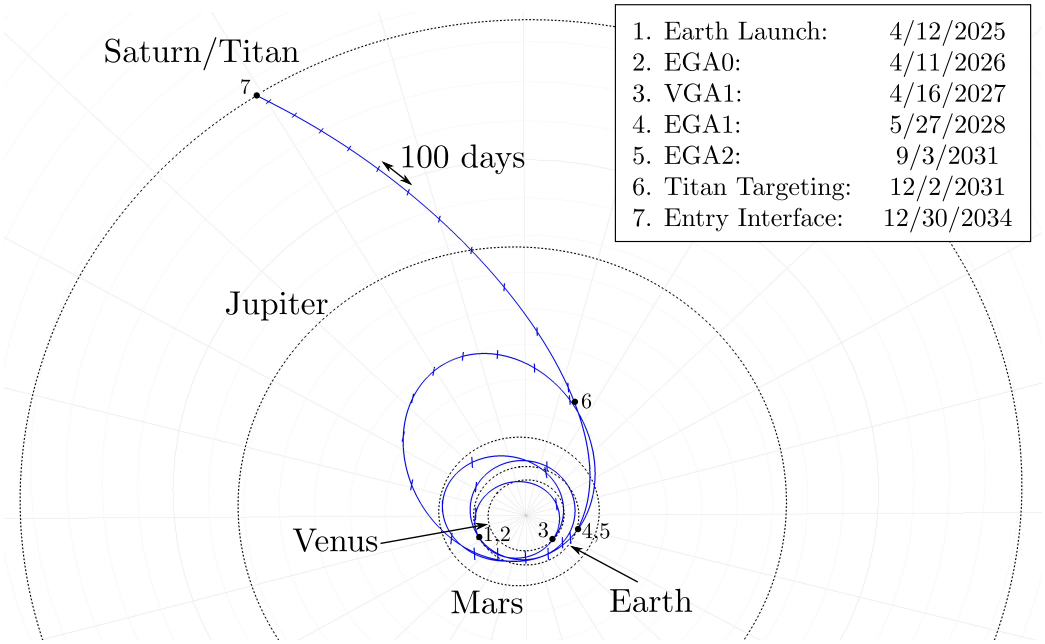

Figure 6. Interplanetary trajectory for the primary 2025 EVEE pathway to Titan. The numbers indicate each sequential encounter body or maneuver in the sequence.

can be modified to within plus or minus a half orbital period of Titan, P_T, with only trivial changes in the corresponding interplanetary trajectory. The time of Titan entry is then bounded by,

$$t_o - \frac{1}{2}P_T < t_e < t_o + \frac{1}{2}P_T \tag{3}$$

where t_o is the nominal arrival time (measured as the time of Saturn periapse passage without Titan entry). The orbit of Titan is discretized into n segments in time which can be mapped to a phasing angle, β, measured from the incoming asymptote direction projected into Titan's orbital plane, $\hat{\mathbf{v}}_{\infty xy}$. Considering an arbitrary entry time t_e the necessary value of node radius, r_N, and phase angle, β, can be found from Titan's ephemeris. Then considering one of either pre- or post-Saturn periapsis encounters and either a pro- or retrograde solution about Saturn, the six classical orbital elements can be fully determined for a given r_p. Each feasible value of r_p will map to a specific value of β. Thus, a simple 1-dimensional root solve can be performed to find the value of r_p necessary for a Titan entry at time t_e.

$$\beta\left(r_p\right) - \beta\left(t_e\right) = 0 \tag{4}$$

The space of all Titan intercepting trajectories corresponding to the chosen interplanetary trajectory is plotted in Figure 7. The entry velocity is independent of latitude and longitude for each trajectory and is shown in Figure 8 along with the Earth sub-latitude and longitude. Considering only prograde Saturnian orbits, each reachable point on Titan's surface will have entry conditions characterized by a corresponding EFPA for a given entry time. Since Titan is tidally locked the point where the incoming Saturn-centered hyperbola intercepts its trajectory directly maps to the region of its surface available for landing.

Target Latitude and Longitude

We define two altitudes which will be important to the following developments. The first is the entry interface altitude, 1,270 km, above which the effects of the atmosphere are negligible and where the entry velocity and EFPA constraints are set. The second is the landing site target altitude,100 km, which serves as a convenient heuristic to map the arrival geometry to the landing site. If this altitude can be reached ballistically

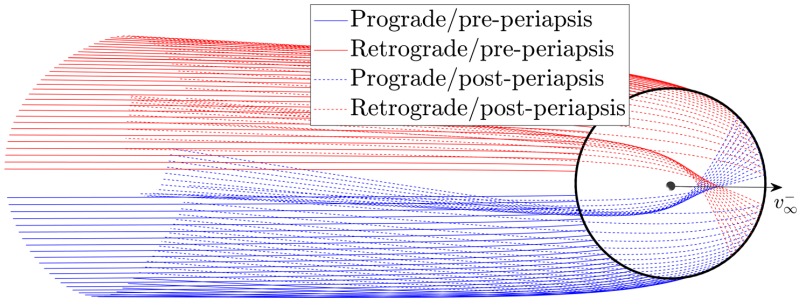

Figure 7. Trajectories entering the Saturnian system for the nominal interplanetary trajectory.

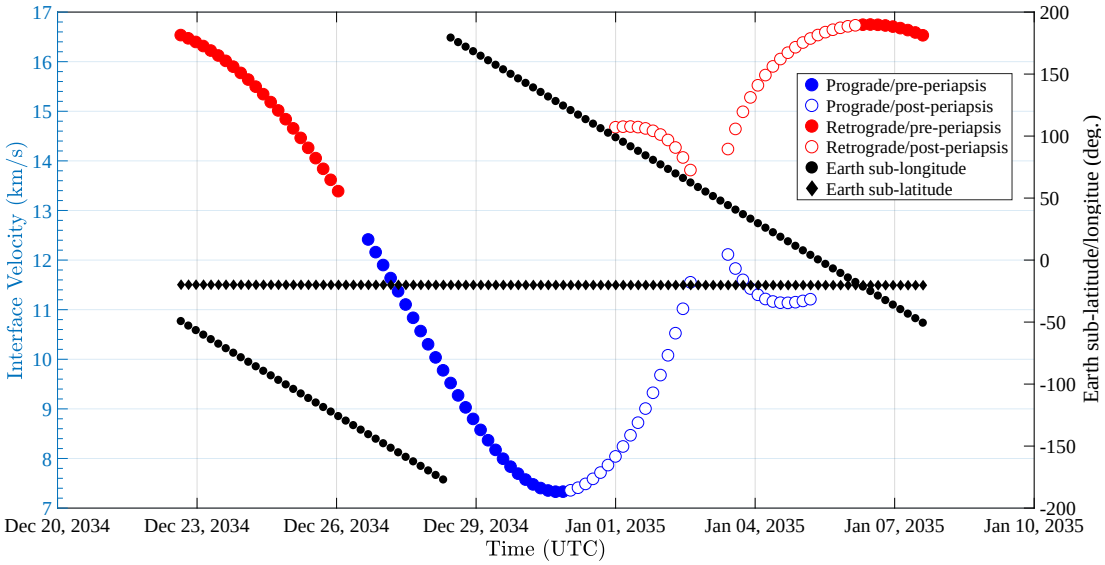

Figure 8. Titan entry velocity at an atmospheric interface altitude of 1,270 km and sub-Earth latitude and longitude versus time.

while satisfying all constraints, then the landing site is assumed to be reachable by the entry system. More detailed analyses are used to refine the targeting. Note that a Titan radius of 2,575 km is assumed for all calculations.

A local coordinate system whose x-axis points in the direction of the target location on the surface is convenient for the following developments. Letting $\mathbf{S}_b = \left[\begin{array}{ccc} \hat{\mathbf{i}}_b & \hat{\mathbf{j}}_b & \hat{\mathbf{k}}_\mathbf{b} \end{array} \right]^T$ be composed of the unit vectors of the Titan-fixed body frame, the transformation to the local coordinate system defined by $\mathbf{S}_l = \left[\begin{array}{ccc} \hat{\mathbf{i}}_l & \hat{\mathbf{j}}_l & \hat{\mathbf{k}}_l \end{array} \right]^T$ becomes,

$$\mathbf{S}_l = C_{l/b}\mathbf{S}_b \tag{5}$$

where

$$C_{l/b} = \left[\begin{array}{ccc} \cos\lambda & \cos\lambda\sin\phi & \sin\lambda \\ -\sin\phi & \cos\phi & 0 \\ -\sin\lambda\cos\phi & -\sin\lambda\sin\phi & \cos\lambda \end{array} \right] \tag{6}$$

and a Titan body-fixed frame described in the report of the IAU/IAG working group is used.[14] If the direction-

cosine matrix from an inertial frame to the Titan-fixed frame is $C_{b/I}$, then the v_∞ of the spacecraft with respect to this local frame is

$$\mathbf{v}_{T\infty l} = C_{l/b} C_{b/I} \mathbf{v}_{T\infty} \tag{7}$$

The goal is to find orbital elements consistent with this asymptote which reach the atmospheric interface altitude above the target latitude and longitude. A process similar to the Saturnian system entry is followed where the node crossing radius in the local frame is set to the atmospheric entry radius. Following the equations in the Appendix there is one degree of freedom available, r_p, to control the latitude and longitude of the interface condition. By construction, if the y-component of the state vector in the local frame, y_{loc}, is zero for a given r_p then the spacecraft reaches the target altitude above the target latitude and longitude if a solution exists. Thus, the problem reduces to a 1-dimensional root solve,

$$y_{loc}\left(r_p\right) = 0 \tag{8}$$

Constraints Based on Orbital Geometry

An altitude, spacecraft sub-latitude, λ, and sub-longitude, ϕ, are the spherical coordinates that are typically used to specify the position vector at atmospheric interface. The locus of all reachable points in terms of latitude and longitude for a specific altitude depends on both the direction and magnitude of $\mathbf{v}_{T\infty}$. Expressing this vector in the Titan-fixed frame

$$\mathbf{v}_{T\infty b} = C_{b/I} \mathbf{v}_{T\infty} \tag{9}$$

It is instructive to identify the sub-latitude and longitude of $\mathbf{v}_{T\infty}$ on both the near and far side of Titan's globe. If the longitude is measured positively counter-clockwise from the x-axis in the body-fixed frame,

$$\begin{array}{rcc} \lambda_f & = & \arcsin\left(\frac{v_{T\infty bz}}{v_{T\infty}}\right) \\ \phi_f & = & \arctan\left(v_{T\infty by}, v_{T\infty bx}\right) \\ \lambda_n & = & -\lambda_f \\ \phi_n & = & \phi_f + \pi \end{array} \tag{10}$$

where the appropriate quadrant check is performed for the longitude and the subscripts 'n' and 'f' denote the near and far side, respectively.

The degenerate case occurs when every point on Titan's globe is reachable. In this case a parabolic orbit reaches periapsis at the required altitude at a sub-latitude and longitude of λ_f and ϕ_f. All other locations at the same altitude are reached prior to periapsis. All realistic cases will have geometrically inaccessible portions of Titan's globe centered about ϕ_f and λ_f. The area of this region varies inversely with the bend angle, Δ_T, of the incoming hyperbola about Titan,

$$\sin\left(\frac{\Delta_T}{2}\right) = \frac{1}{e_T} \tag{11}$$

where the eccentricity about Titan can be expressed as

$$e_T = 1 + \frac{r_{pT} v_{T\infty}^2}{\mu} \tag{12}$$

r_{pT} is the radius of periapsis set by the target altitude. Using the formula for the surface area of a spherical cap and Eq. 11, the fraction of Titan's surface which is accessible can be expressed as

$$\frac{1}{2}\left(1 + \frac{1}{e_T}\right) \tag{13}$$

Constraints Derived from the Entry System

The peak deceleration, heat flux, and heat load for the entry vehicle are functions of both the velocity and EFPA at the entry interface altitude. In general for a given entry interface velocity, the peak deceleration and heat flux increases as the magnitude of the EFPA is increased. Thus, a maximum EFPA magnitude, $|\gamma|_{max}$, can be identified consistent with the constraints outlined in Table 1. There is also a minimum bound on the EFPA magnitude, $|\gamma|_{min}$, which corresponds to a trajectory that does not have adequate time to dissipate its energy within the atmosphere to reach the surface. Figure 9 shows the inaccessible regions on a cross-section of Titan's globe. The fraction of Titan's surface which is accessible is then,

$$\frac{1}{2}\left(\cos\kappa_1 - \cos\kappa_2\right) \tag{14}$$

where

$$\kappa_{1,2} = \frac{1}{2}\left(\pi - \Delta_{1,2}\right) - \theta_{1,2} \tag{15}$$

Here $\theta_{1,2}$ are the absolute values of true anomaly at the target altitude set by the lower and upper bounds of the EFPA at the interface altitude. $\Delta_{1,2}$ are the bend angles of the hyperbola corresponding to these bounding orbits. $\kappa_{1,2}$ can be calculated using the following well-known relationships

$$\begin{aligned} h_{1,2} &= r_I v_I \cos|\gamma|_{min,max} \\ e_{1,2} &= \sqrt{1 - \tfrac{h_{1,2}}{\mu a}} \\ \cos\theta_{1,2} &= \tfrac{h_{1,2}^2}{\mu r_T e_{1,2}} - \tfrac{1}{e_{1,2}} \end{aligned} \tag{16}$$

where r_I and v_I are the position and velocity vector magnitudes at the entry interface and r_T is the position vector magnitude at the target altitude.

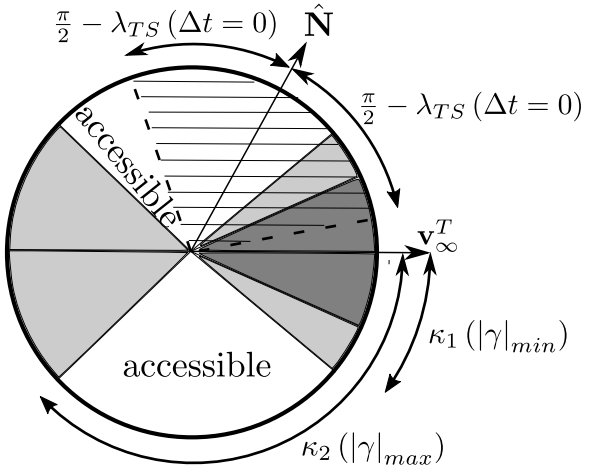

Figure 9. Cross-section of Titan's globe with the accessible regions shown in white. The regions shown in light and dark gray correspond to inaccessible regions due to EFPA and geometric constraints of the incoming hyperbola, respectively. The hatched region shows areas in terms of latitude which can not meet the minimum time to Earthset requirement.

Time to Earthset

The previous sections have identified points on the surface that are both geometrically accessible by an incoming trajectory and physically reachable by a flight system with bounds on the entry interface velocity and EFPA. An additional Earth-access constraint is placed on the mission that ensures ample time for system check-out and initial science operations after landing. The analysis found in Appendix,shows that for a finite

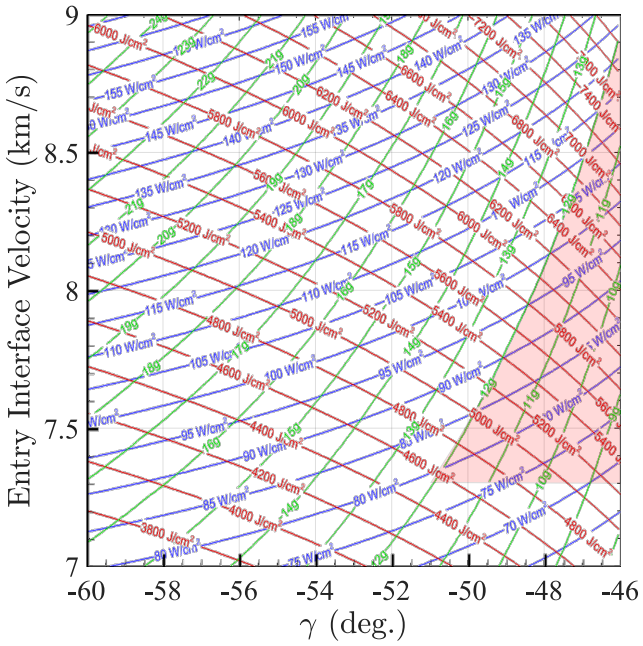

Figure 10. Entry acceleration and representative heat load/flux conditions. The shaded area corresponds to the design space encompassed by the nominal interplanetary trajectory and falls comfortably within the bounds listed in Table 1. Graphic courtesy of Aaron Brandis and Gary Allen at NASAs Ames Research Center.

earth declination relative to Titan's equatorial plane at least one continuous region of latitude values centered about the north or south poles never has Earth access. If a declination constraint on antenna pointing relative to the local horizon is introduced (corresponding to values of $\Theta_{max} < 90°$) then two bands of latitudes without Earth access centered about the north and south poles can exist depending on the Earth declination. The longitude band which satisfies the Earth-access constraint depends on the time of entry in addition to the Earth declination and pointing constraint. Figure 9 shows the general geometry relevant to Dragonfly. The scientific choice of landing site within the accessible region will be discussed elsewhere.

DESIGN SPACE AND SAMPLE ENTRY

For all entry times, a maximum deceleration value of 12g's is used as an upperbound for the design of the entry system. This value sets the maximum absolute value of the EFPA, $|\gamma|_{max}$, as shown in Figure 10. The lower absolute bound on EFPA, $|\gamma|_{min}$, is conservatively set to the value which renders ballistically reaching the target altitude impossible. This value is approximately $45°$, for the range of entry interface velocities highlighted in Figure 10.

The nominal interplanetary trajectory design corresponds to a Titan entry time with a low entry velocity, relative to the rest of the design space. In a high-fidelity model the spacecraft arrives at Titan on December 30, 2034 15:13:13 UTC with $\mathbf{v}_{\infty T} = [-0.910, 5.081, 4.710]^T$ km/s. This vector translates into a velocity of 7.3 km/s at the entry interface altitude. The maximum deceleration and thermal conditions at this velocity upon entry can be found in Figure 10. A maximum deceleration value of 12g's corresponds to a maximum absolute value of the EFPA of approximately $51°$ with the minimum bound at approximately $45°$. Figure 11 shows the build up of the inaccessible region based on the geometry of the hyperbolic orbit, EFPA constraints, and time to Earthset constraint in that order. Table 5 shows the reduction in accessible surface area with the addition of each constraint.

Using the developments in Appendix and imposing no Earth declination constraints ($\Theta_{max} = \pi/2$) for

the time period of interest, the latitude range which yields no Earth access is approximately 72 to 90 deg. Conversely, latitudes from -90 to -72 deg. yield continuous access. Of particular interest is the latitude range for which the minimum time to Earthset can be satisfied. This range is -90° to 67°, using Eq. 45. These results are summarized in Table 4.

Table 4. Summary of Earth access regions in terms of latitude for the nominal interplanetary trajectory.

Access Type	Latitude Bounds	Calculation
No Access	72° to 90°	Equation 41
Continuous Access	-90° to -72°	Equation 40
Constraint Satisfaction Possible	-90° to 67°	Equation 44

Table 5. Percent of accessible surface with constraint additions for the nominal case.

Constraints	Accessible Surface Fraction	Calculation
Hyperbolic Geometry	53%	Equation 13
Hyperbolic Geometry+EFPA Constraints	22%	Equation 14
Hyperbolic Geometry+EFPA Constraints +Earthset Constraint	7%	Numerical Integration

As the nominal entry time is moved backwards or forwards the entry velocity increases which decreases the accessible region on the surface before the Earthset constraint is considered. The accessible region also shifts relative to the surface as Titan rotates ($22.6^\circ/$ day) and the direction of $\mathbf{v}_{T\infty}$ changes inertially. These changes over a period of 1.5 Earth days are shown in Figure 12.

As an illustrative example, we show the entry sequence corresponding to the second arrival point in Figure 12 starting with the Saturnian system arrival. In this case, a target latitude and longitude of 22° and 100° specify a point that lies on the edge of the design space with an interface velocity of 7.5 km/s, corresponding to maximum deceleration 12 g's and EFPA of -50°. Note that the interface point is reached prior to crossing the equatorial plane of Titan, as seen in Figure 13.

NAVIGATION

The maneuvers are predominantly driven by statistical factors with the mission Δv budget for the preliminary design appearing in Table 6. With the exception of the deep space maneuver (DSM) to maintain a fixed Titan entry state vector, all other maneuvers are either purely statistical or deterministically driven by statistical factors. Since the baseline mission concept is powered by a MMRTG, each Earth gravity assist must require a biased aimpoint such that the impact probability is sufficiently low. The biasing analysis will be documented in a future publication. This section presents the preliminary $\Delta v99$ results which are currently being refined in conjunction with Earth-biasing.

This analysis is accomplished via a statistical process that accounts for errors in determining the orbit of the spacecraft as well as errors in executing trajectory correction maneuvers (TCMs) needed to maintain a reference trajectory.[15] For a trajectory with planetary gravity assists, it is especially important to maintain close adherence to the reference trajectory at the time of each flyby since offsets from the nominal flyby condition will be amplified on the following leg. To manage these navigation errors, we devised a series of trajectory correction maneuvers (TCMs) consisting of three maneuvers approaching each flyby and one cleanup maneuver following each flyby. The approach maneuvers (with some exceptions) are scheduled for 90, 30, and 10 days prior to each flyby, and the cleanup maneuver is placed 20 days following each flyby.

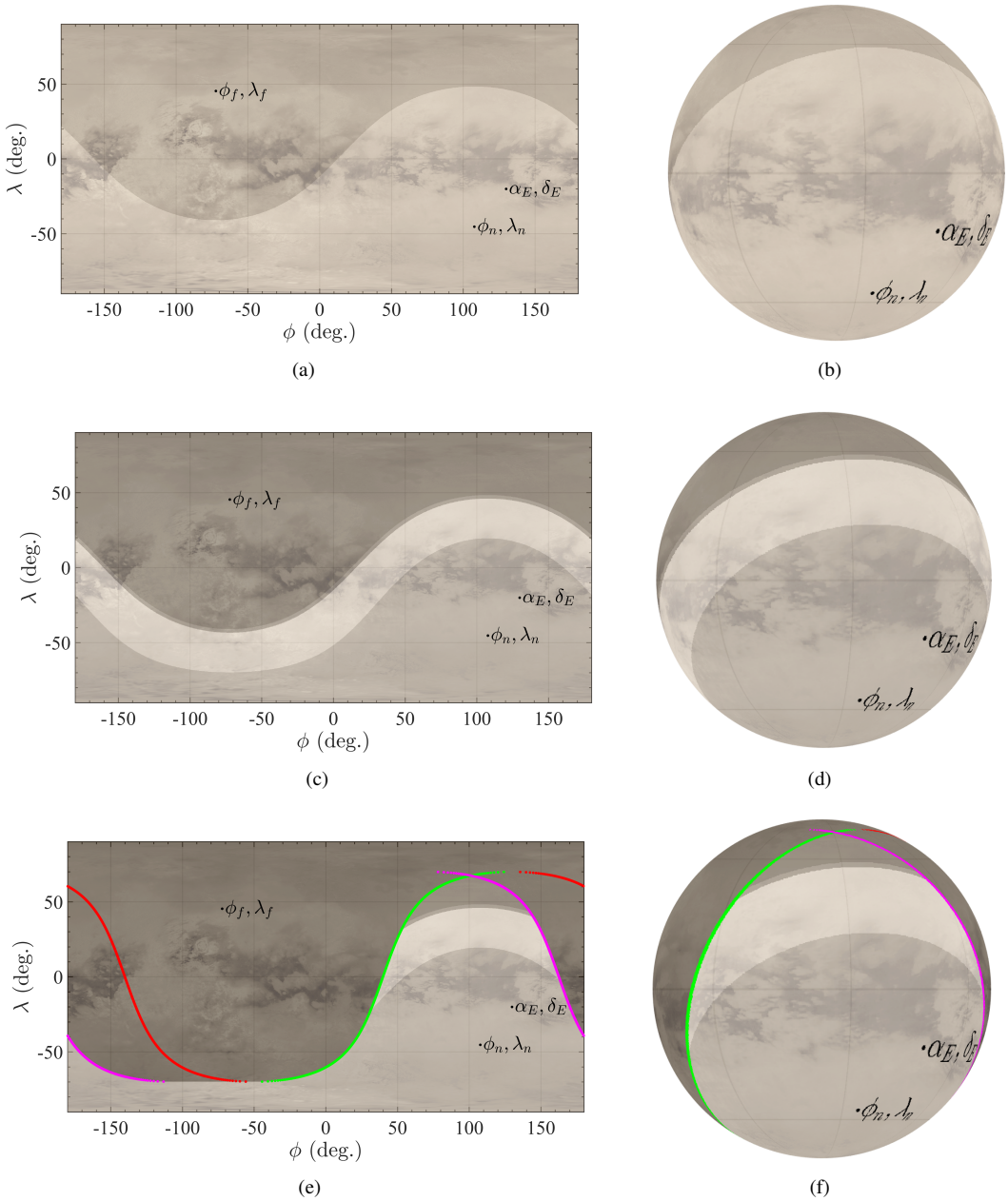

Figure 11. Build-up of inaccessible regions for the nominal entry time. The Earth's sub-longitude, -latitude (ϕ_E, λ_E) and the near and far projections of the v_∞ vector ($\phi_{n,f}$, $\lambda_{n,f}$) are shown. The brightest region on each map is accessible with view point looking down approximately at the trailing edge for the globes and the sub-Saturn point for the 2D maps. (a) Geometrically accessible latitude and longitude of incoming hyperbola; (b) Geometrically accessible latitude and longitude on globe; (c) Accessible region with EFPA constraints; (d) Accessible region with EFPA constraints on globe; (e) Accessible region with Earthset constraint. The green and red lines correspond to Earthrise and Earthset, respectively. The magenta line corresponds to Earthset line shifted by the 61 hr. constraint.; (f) Accessible region with Earthset constraint on globe.

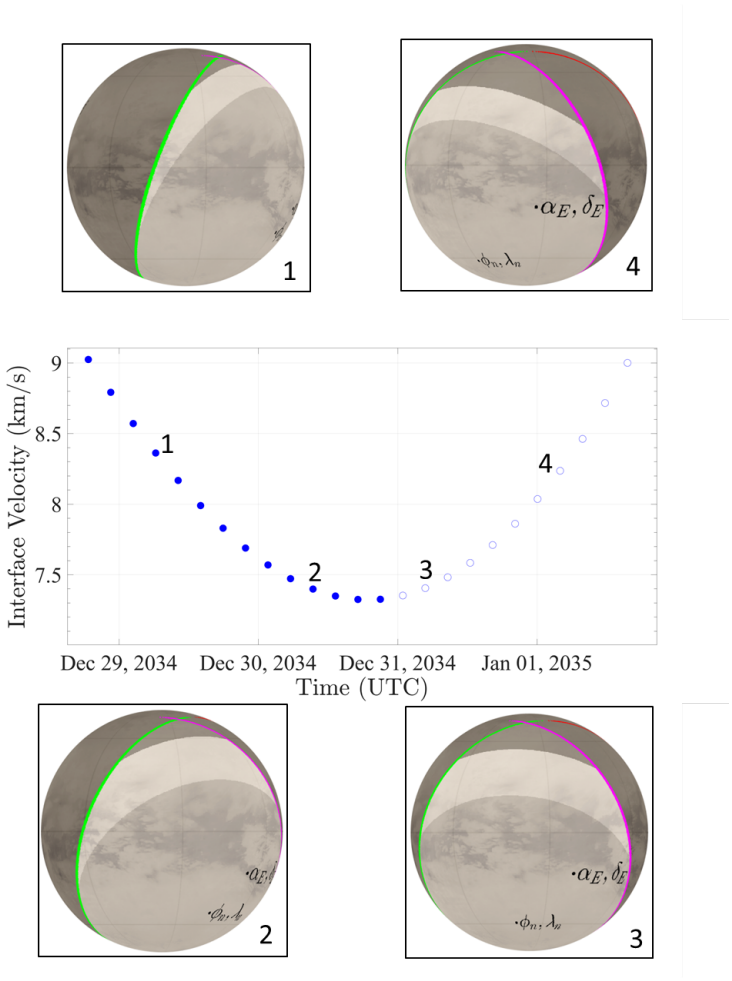

Figure 12. Change in accessible surface area versus time and as a function of entry interface velocity. The filled and open circles represent Titan entry before the spacecraft has passed periapsis with respect to Saturn and after it has passed periapsis, respectively. The viewpoint is stationary above the trailing edge of Titan. Proceeding in order with time, the fraction of the accessible surface is 4%, 6%, 7%, and 5% considering all constraints.

In addition, there is a launch cleanup maneuver 15 days after launch, and the E1 to E2 transfer has an extra maneuver 800 days prior to the E2 flyby to prevent errors from building over this longer transfer. The E2 to Titan leg has a post-E2 cleanup 60 days after the flyby. TCMs targeting the Titan arrival are scheduled for 548, 45, 15, 5, and 2 days prior to landing.

The process used to obtain an estimate of the uncertainty in the orbit is a standard covariance analysis.[16] Simulated tracking data is used in a least squares filter which provides the covariance of the orbit estimate at the time of each TCM data cutoff (5 days before each TCM). The simulated tracking data includes range and range rate measurements, and the estimated parameters in the filter include the position and velocity of the spacecraft, as well as parameters related to the dynamical model of the trajectory and error sources. A Monte Carlo technique is applied which samples a trajectory, first from the dispersions due to the delivery to the injection state from the launch vehicle, and subsequently from errors in determining the orbit of the spacecraft. For each sample, a TCM is designed using the linearized state transition matrix to compute the Δv required to remove the error at the time of the next flyby. Maneuver execution errors are also added to each TCM. The process is repeated n times to obtain statistics on the mean, standard deviation, and 99th

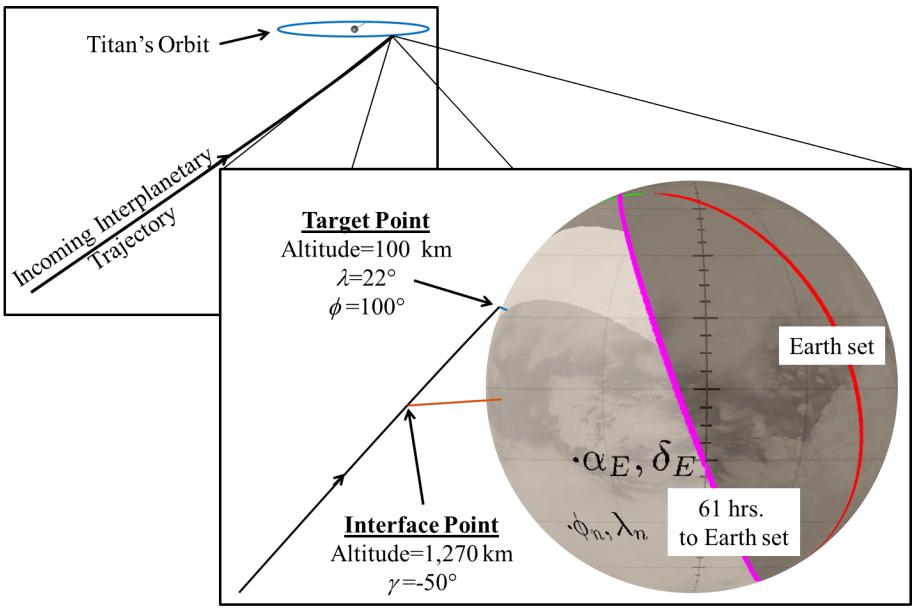

Figure 13. A typical entry geometry corresponding to the second arrival point in Figure 12.

percentile of the size of the maneuvers needed. The results of this analysis are shown in Table 7. For these results, 5000 samples were used in the Monte Carlo simulation, and 99% of these samples required not more than 95 m/s of Δv to adhere to the reference trajectory. Note that this estimate of the statistical maneuvers is 30 m/s greater than the initial estimate listed in 6. Further refinements to the process will be made in conjunction with the biasing analysis moving forward.

CONCLUSIONS

Dragonfly has a simple interplanetary design consisting of at most one deterministic maneuver (excluding biasing maneuvers), and sometimes none would be required throughout the launch period. This single maneuver allows the spacecraft to enter Titan's atmosphere at the exact time and state through both the primary and backup launch periods, greatly simplifying operational planning. Upon entry into the Saturnian system Dragonfly would have access to a wide region of Titan's northern hemisphere and areas of the southern hemisphere with small adjustments in the entry time. Overall, these attributes constitute a mission concept design that is both flexible to surface targets and robust to launch delays. Future publications will address the navigation of the spacecraft which includes the ongoing $\Delta v99$ analysis and the Earth biasing study, which is necessary for a spacecraft with a nuclear payload.

ACKNOWLEDGMENTS

The authors wish to thank the Dragonfly Principal Investigator, Elizabeth Turtle, for her contributions to the development of the baseline mission design. The authors would like to express our appreciation to Aaron Bandis and Gary Allen of NASA Ames for the production of Figure 10 and Robert Maddock, Joseph White, and Richard Winski of LaRC for their support throughout the project. The authors would also like to thank Sumita Nandi and Zahi Tarzi of JPL for the initial navigation studies of the step 1 proposal and Jim McAdams for his mission design work in the earlier stages of the project. Part of the research described in this paper was performed at the Jet Propulsion Laboratory, California Institute of Technology, under contract with the National Aeronautics and Space Administration. The information presented about the Dragonfly mission concept is pre-decisional, and is provided for planning and discussion purposes only.

Table 6. Dragonfly interplanetary Δv budget for the preliminary design. Statistical maneuvers are estimated.

Maneuver	Total Δv (m/s)	Deterministic Δv (m/s)	Statistical Δv (m/s)	Comment
1. Launch Cleanup	20.0	0.0	20.0	Typical value, pending Phase A analysis
2. EGA0 (Bias and Targeting)	50.0	40.0	10.0	Estimate pending further analysis
3. VGA1 (Bias and Targeting)	10.0	0.0	10.0	Estimate pending further analysis
4. EGA1 (Bias and Targeting)	50.0	40.0	10.0	Estimate pending further analysis
5. EGA2 (Bias and Targeting)	50.0	40.0	0.0	Estimate pending further analysis
6. DSM for fixed Titan state (at EGA2+90 days)	20.7	20.7	10.0	Worst case over launch period
7. Titan Targeting	10.0	0.0	10.0	
Subtotals	210.7	140.7	70.0	
Contingency	7.0	0.0	7.0	Unforeseen scenarios, 5% of deterministic
Grand Total	217.7			Deterministic + statistical + contingency

REFERENCES

[1] R. D. Lorenz *et al.*, "Dragonfly: A Rotorcraft Lander Concept for Scientific Exploration at Titan," *Johns Hopkins APL Technical Digest*, 2018.

[2] L. Less *et al.*, "The Tides of Titan," *Science*, Vol. 337, 2012, pp. 457–459.

[3] F. Raulin, C. McKay, J. Lunine, and T. Owen, *Titans Astrobiology*. Springer, 2010.

[4] R. D. Lorenz, "Post-Cassini Exploration of Titan: Science Rationale and Mission Concepts," *JBIS*, Vol. 53, 2000, pp. 218–234.

[5] E. Stofan, R. Lorenz, J. Lunine, E. Bierhaus, B. Clark, P. Mahaffy, and M. Ravine, "TiME-The Titan Mare Explorer," *IEEE Aerospace Conference*, Big Sky, MT, March 2013, 10.1109/AERO.2013.6497165.

[6] M. K. Lockwood *et al.*, "Titan Explorer," *AAS/AIAA Astrodynamics Specialist Conference*, Paper No. AAS 2008-7071, Honolulu, HI, Aug 2008, 10.2514/6.2008-7071.

[7] *Planetary Science Decadal Survey: Titan Saturn System Mission*. 2010.

[8] D. Lantukh, R. Russell, and S. Campagnola, "V-Infinity Leveraging Boundary-Value Problem and Application in Spacecraft Trajectory Design," *Journal of Spacecraft and Rockets*, Vol. 52, No. 3, 2015, pp. 697–710, 10.2514/1.A32918.

[9] N. Strange, R. Russell, and B. Buffington, "Mapping the V-Infinity Globe," *AAS/AIAA Astrodynamics Specialist Conference*, Paper No. AAS 07-277, Mackinac Island, Michigan, August 9-13,2007.

[10] J. Atchison, M. Ozimek, C. Scott, and F. Siddique, "Robust High-Fidelity Gravity-Assist Trajectory Generation Using Forward/Backward Multiple Shooting," *AAS/AIAA Space Flight Mechanics Meeting*, Paper No. AAS 15-249, Williamsburg, Virginia, January 11-15,2015.

[11] C. Ocampo, J. Senent, and J. Williams, "Theoretical Foundation of Copernicus: A Unified System for Trajectory Design and Optimization," *4th International Conference on Astrodynamics Tools and Techniques*, Madrid, Spain, May 3-6,2010.

[12] W. Taber, T. Drain, J. Smith, H.-C. Wu, M. Guevara, R. Sunseri, and J. Evans, "MONTE: The Next Generation of Mission Design and Navigation Software," *CEAS Space Journal*, Vol. 10, No. 1, 2018, pp. 79–86, 10.1007/s12567-017-0171-7.

[13] C. J. Scott, M. T. Ozimek, A. F. Haapala, F. E. Siddique, and B. B. Buffington, "Dual Satellite-Aided Planetary Capture with Interplanetary Trajectory Constraints," *Journal of Guidance, Control, and Dynamics*, Vol. 40, No. 3, 2017, pp. 548–562, 10.2514/1.G002102.

[14] B. A. Archinal *et al.*, "Report of the IAU/IAG Working Group on Cartographic Coordinates and Rotational Elements: 2009," *Celestial Mechanics*, Vol. 109, 2011, pp. 101–135, 10.1007/s10569-010-9320-4.

[15] E. H. Maize, "Linear Statistical Analysis of Maneuver Optimization Strategies," *AAS/AIAA Astrodynamics Specialist Conference*, Kalispell, MT. August 22-25, 1987.

[16] T. J. Martin-Mur, R. Ionasescu, P. Valerino, K. Criddle, and R. Roncoli, "Navigational challenges for a Europa flyby mission," *24th International Symposium on Space Flight Dynamics*, Laurel, MD May 5-9, 2014.

Table 7. Updated Statistical Maneuver Δv Budget

TCM	Date	Mean ΔV, m/s	1-σ, m/s	99%tile, m/s
0	27-APR-2025	2.915e+00	2.131e+00	9.241e+00
1	11-JAN-2026	6.713e-01	7.251e-01	3.532e+00
2	12-MAR-2026	9.297e-02	7.572e-02	3.944e-01
3	01-APR-2026	4.042e-02	1.733e-02	8.670e-02
4	01-MAY-2026	4.604e+00	3.544e+00	1.641e+01
5	16-JAN-2027	5.078e-01	5.367e-01	2.663e+00
6	17-MAR-2027	8.570e-02	6.750e-02	3.437e-01
7	06-APR-2027	4.393e-02	1.900e-02	9.518e-02
8	06-MAY-2027	5.774e+00	4.210e+00	1.993e+01
9	27-FEB-2028	1.904e+00	2.149e+00	9.927e+00
10	27-APR-2028	1.887e-01	2.162e-01	1.085e+00
11	17-MAY-2028	4.803e-02	2.316e-02	1.250e-01
12	16-JUN-2028	7.000e+00	5.639e+00	2.772e+01
13	25-JUN-2029	4.355e-01	4.727e-01	2.451e+00
14	05-JUN-2031	9.767e-01	7.542e-01	3.380e+00
15	04-AUG-2031	1.126e-01	9.092e-02	4.392e-01
16	24-AUG-2031	3.995e-02	1.741e-02	8.733e-02
17	02-NOV-2031	3.644e+00	3.030e+00	1.538e+01
18	30-JUN-2033	3.262e-01	3.050e-01	1.557e+00
19	15-NOV-2034	5.292e-01	2.316e-01	1.150e+00
20	15-DEC-2034	6.539e-02	3.197e-02	1.620e-01
21	25-DEC-2034	2.738e-02	1.164e-02	5.880e-02
22	28-DEC-2034	6.913e-03	2.993e-03	1.480e-02
Total		30.04	18.48	95.16

[17] B. Wie, *Space Vehicle Dynamics and Control*. American Institude of Aeronautics and Astronautics, Inc., 1998.

APPENDIX

Titan Excess Velocity

Using the orbit equation, the true anomaly of the spacecraft at a node is

$$\theta_N = \left\{ \begin{array}{cc} \arccos\left(\frac{p}{er_N} - \frac{1}{e}\right) & (\text{Titan entry after Saturn periapsis}) \\ -\arccos\left(\frac{p}{er_N} - \frac{1}{e}\right) & (\text{Titan entry before Saturn periapsis}) \end{array} \right\} \tag{17}$$

where R_N is the radius of the node, p is the semi-parameter, and e is the eccentricity about Saturn. Here e and p are known as v_∞ is set by the interplanetary trajectory and r_p is chosen a priori. The argument of periapsis is

$$\omega = \left\{ \begin{array}{cc} -\theta_N & (\text{Titan entry at ascending node}) \\ \pi - \theta_N & (\text{Titan entry at descending node}) \end{array} \right\} \tag{18}$$

and the radius at the node is

$$R_N = \left\{ \begin{array}{cc} \frac{p}{1+e\cos(-\omega)} & (\text{Titan entry at ascending node}) \\ \frac{p}{1+e\cos(\pi-\omega)} & (\text{Titan entry at descending node}) \end{array} \right\} \tag{19}$$

Because $R_N > 0$, the existence of the nodes is given as follows:

$$\begin{array}{rcc} \cos\omega > -\frac{1}{e} & : & \text{Titan entry possible at ascending node} \\ \cos\omega < \frac{1}{e} & : & \text{Titan entry possible at descending node} \\ -\frac{1}{e} < \cos\omega < \frac{1}{e} & : & \text{Entry possible at both ascending and descending nodes} \end{array} \tag{20}$$

The incoming asymptote is connected to the orbital elements of the hyperbola using the standard perifocal frame, $\hat{\mathbf{p}}$-$\hat{\mathbf{q}}$-$\hat{\mathbf{w}}$, as

$$\mathbf{v}_\infty^{pqw} = P\left(\Omega, \omega, i\right) \mathbf{v}_\infty \tag{21}$$

where P is given by the standard conversion.[17] Here, Ω and i are the right ascension of the ascending node and inclination with respect to the Saturn, respectively. The velocity $\mathbf{v}_\infty^{pqw}$ is obtained via the true anomaly at negative infinity.

It follows from Eqs. 1 and 21

$$\sin i = \frac{v_\infty \sin\delta}{v_{\infty y}^{pqw}\cos(\omega) + v_{\infty x}^{pqw}\sin(\omega)} = \frac{\sin\delta}{\cos\left(\omega + \arctan\left(-\frac{v_{\infty x}^{pqw}}{v_{\infty y}^{pqw}}\right)\right)} \tag{22}$$

where the quadrant is chosen in accordance with a prograde or retrograde solution. Similarly

$$\Omega = \alpha - \arcsin\left(\frac{\tan(\delta)}{\tan(i)}\right) = \alpha + \arccos\left(\frac{v_{\infty x}^{pqw}\cos(\omega) - v_{\infty y}^{pqw}\sin(\omega)}{v_\infty \cos(\delta)}\right) \tag{23}$$

A quadrant check is performed by comparing the two expressions in equation 23.

The radius and velocity vectors at the node are now computed as

$$\begin{aligned} \mathbf{r}_N &= P^T \mathbf{r}_N^{pqw} \\ \mathbf{v}_N &= P^T \mathbf{v}_N^{pqw} \end{aligned} \tag{24}$$

where

$$\begin{aligned} \mathbf{r}_N^{pqw} &= R_N \begin{bmatrix} \cos\theta_N & \sin\theta_N & 0 \end{bmatrix}^T \\ \mathbf{v}_N^{pqw-} &= \sqrt{\frac{\mu}{p}} \begin{bmatrix} \sin\theta_N & e + \cos\theta_N & 0 \end{bmatrix}^T \end{aligned} \tag{25}$$

Thus, the full state at the node is defined analytically.

The incoming v_∞ vector relative to Titan is defined provided that the state of Titan at the first node is known. A fully analytical expression can be found if Titan's orbit is assumed to be circular. However, for the purpose of this study JPL Spice ephemerides are used for increased accuracy. The incoming excess velocity relative to the Titan is

$$\mathbf{v}_{T\infty} = \mathbf{v}_N - \mathbf{v}_T \tag{26}$$

where $\mathbf{v}_T$ is the velocity of Titan relative to Saturn.

Time to Earthset

Expressing the inertial Earth direction from Titan $\hat{\mathbf{n}}_E$ in the Titan body frame,

$$\hat{\mathbf{n}}_E = C_{I/b}\hat{\mathbf{n}}_{Eb} \tag{27}$$

where the superscript "I" indicates the time derivative in an inertial frame. Therefore the velocity of the unit vector as seen from the Titan-fixed frame is,

$$\dot{\hat{\mathbf{n}}}_{Eb} = \dot{\hat{\mathbf{n}}}_{Eb}^I - C_{b/I}\dot{C}_{b/I}\hat{\mathbf{n}}_{Eb} \tag{28}$$

This expression is convenient for operating on the DCM directly. If it is also assumed that the Titan body frame rotates with an angular velocity with respect to the inertial frame, $\boldsymbol{\omega} = \begin{bmatrix} \omega_x & \omega_y & \omega_z \end{bmatrix}$, then by the kinematic transport theorem, the definition of cross product

$$\dot{\hat{\mathbf{n}}}_{Eb} = \dot{\hat{\mathbf{n}}}_{Eb}^I - \boldsymbol{\omega}_b \times \hat{\mathbf{n}}_{Eb} = \dot{\hat{\mathbf{n}}}_{Eb}^I - \Omega_b \hat{\mathbf{n}}_{Eb} \tag{29}$$

If it is assumed that the Titan rotation axis is inertially fixed within plus or minus a half orbital period and that the z-axis of the inertial frame is aligned with axis of rotation then $C_{b/I}$ takes the form of the standard right-handed, direction-cosine-matrix. Also assuming that rotation rate and inertial Earth direction is constant over plus or minus a half orbital period and defining

$$\hat{\mathbf{n}}_{Eb} = \begin{bmatrix} n_{Ebx} & n_{Eby} & n_{Ebz} \end{bmatrix}^T \tag{30}$$

then

$$\dot{\hat{\mathbf{n}}}_{Eb} = \begin{bmatrix} \omega_b n_{Eby} & -\omega_b n_{Ebx} & 0 \end{bmatrix}^T \tag{31}$$

where

$$\theta(t) = \omega_b (t - t_e) \tag{32}$$

Defining the direction of a potential target site in the Titan-body frame,

$$\hat{\mathbf{r}}_{TSb} = \begin{bmatrix} \cos\phi_{TS}\cos\lambda_{TS} & \sin\phi_{TS}\cos\lambda_{TS} & \sin\lambda_{TS} \end{bmatrix}^T \tag{33}$$

and letting the inertial Earth direction be

$$\hat{\mathbf{n}}_E = \begin{bmatrix} \cos\alpha_E\cos\delta_E & \sin\alpha_E\cos\delta_E & \sin\delta_E \end{bmatrix}^T \tag{34}$$

Using the previous relationships it can be shown that $\cos\Theta = \hat{\mathbf{r}}_{TSb} \cdot \hat{\mathbf{n}}_{Eb}$ becomes,

$$\begin{gathered} \cos\Theta = \cos\lambda_{TS}\cos\delta_E\cos(\theta + \phi_{TS} - \alpha_E) + \sin\delta_E\sin\lambda_{TS} \\ \dot{\Theta} = \frac{1}{\sin\Theta}\left(\omega_b\cos\lambda_{TS}\cos\delta_E\sin(\theta + \phi_{TS} - \alpha_E)\right) \end{gathered} \tag{35}$$

This relationship can also be derived using spherical trigonometry. The declination of the Earth with respect to the target site is

$$\delta_{E/TS} = \pi/2 - \Theta \tag{36}$$

For Earth communication the declination must remain above some minimum value, $\delta_{E/TSmin}$, which corresponds to a maximum value of Θ. It can be shown via Eq. 35 or geometrically that for communication to be possible,

$$\Theta_{max} > |\delta_E - \lambda_{TS}| \tag{37}$$

For a given target latitude at the entry time the longitude coordinates corresponding to a given value of Θ is

$$\phi_{TS} = \alpha_E \pm \arccos\left(\frac{\cos\Theta}{\cos\lambda_{TS}\cos\delta_E} - \tan\lambda_{TS}\tan\delta_E\right) \tag{38}$$

The time available at a given latitude below Θ_{max} becomes,

$$\Delta t = \left(\frac{2}{\omega_b}\right)\arccos\left(\frac{\cos\Theta_{max}}{\cos\lambda_{TS}\cos\delta_E} - \tan\lambda_{TS}\tan\delta_E\right) \tag{39}$$

There are two cases of particular interest corresponding to latitudes that mark no access and those that mark continuous access barring other obstructions, corresponding to $\Delta t = 0$ and $\Delta t = 2\pi/\omega_b$. By geometrical inspection if there is a solution where $\Delta t = 2\pi/\omega_b$ then there is one solution where $\Delta t = 0$. Alternatively, if there are no solutions where $\Delta t = 2\pi/\omega_b$ then there are two solutions where $\Delta t = 0$. Thus, if there is a solution to the following equation where $|\lambda_{TS}(\Delta t = 2\pi/\omega_b)| < \pi/2$,

$$\lambda_{TS}(\Delta t = 2\pi/\omega_b) = -\delta_E + \text{sign}(\delta_E)(\pi - \Theta_{max}) \tag{40}$$

then

$$\lambda_{TS}(\Delta t = 0) = \delta_E - \text{sign}(\delta_E)\Theta_{max} \tag{41}$$

or alternatively

$$\lambda_{TS}(\Delta t = 0) = \delta_E \pm \Theta_{max} \tag{42}$$

with the maximum possible time, Δt_{max}, occurring at

$$\lambda_{\Delta t_{max}} = \arcsin\left(\frac{\sin\delta_E}{\cos\Theta_{max}}\right) \tag{43}$$

Upon landing the mission requires minimum duration for Earth contact, Δt_{min}. If there is a solution such that $\Delta t = 2\pi/\omega_b$ then there is at least one latitude where the time to Earthset equals Δt_{min}. Using Eq. 38 and simplifying,

$$\lambda_{t_{min}} = -\text{sign}\left(\delta_E\right) \arccos\left(\cos\left(\frac{\Theta_{max}}{A}\right) - \Delta\right) \tag{44}$$

Alternatively, if there are two latitudes such that $\Delta t = 0$ and if $\Delta t_{min} < \Delta t_{max}$ then there are two latitudes where time to Earthset equals Δt_{min}.

$$\lambda_{t_{min}} = \pm \arccos\left(\cos\left(\frac{\Theta_{max}}{A}\right) - \Delta\right) \tag{45}$$

where

$$A^2 = \cos^2\left(\frac{\omega_b \Delta t_{min}}{2}\right)\cos^2\left(\delta_E\right) + \sin^2\left(\delta_E\right) \tag{46}$$

and

$$\Delta = \arctan\left(\frac{-\sin\left(\delta_E\right)}{\cos\left(\frac{\omega_b \Delta t_{min}}{2}\right)\cos\left(\delta_E\right)}\right) \tag{47}$$